# Temperature-dependent second- and third-order optical nonlinear susceptibilities at the $Si/SiO_2$ interface

Xiong Lu, Robert Pasternak, Heungman Park, Jingbo Qi, and Norman H. Tolk
*Department of Physics and Astronomy, Vanderbilt University, Nashville, Tennessee 37235, USA*

Amitabh Chatterjee, Ronald D. Schrimpf, and Daniel M. Fleetwood
*Department of Electrical Engineering and Computer Science, Vanderbilt University, Nashville, Tennessee 37235, USA*
(Received 22 November 2005; revised manuscript received 8 July 2008; published 13 October 2008)

Using a two-color laser technique, we have measured the temperature dependence of the second- and third-order optical nonlinear susceptibilities, $\chi^{(2)}$ and $\chi^{(3)}$, at the $Si/SiO_2$ interface. A laser beam at 540 nm directed normal to the surface was used to pump electrons from the silicon valence band to trap states on the $SiO_2$ surface leaving the holes at or near the interface thus creating a capacitance electric field. A second beam of wavelength 800 nm incident at 45° on the same spot resulted in a second-harmonic signal whose intensity was related to the varying interfacial electric field. We find that the photoinduced electric field is temperature independent since the charge distributions remain unchanged after pumping and both $\chi^{(2)}$ and $\chi^{(3)}$ increase as the temperature increases.

DOI: 10.1103/PhysRevB.78.155311 PACS number(s): 42.65.An, 42.65.Ky, 31.70.Hq, 32.80.Wr

## I. INTRODUCTION

Second-harmonic (SH) generation (SHG) was shown to be a sensitive probe of the electric field at buried semiconductor interfaces.[1–5] In particular, electric-field-induced second-harmonic (EFISH) generation arising from internal photoemission has been used widely for fundamental studies of charge-carrier dynamics in semiconductor or insulator systems.[6,7] This class of measurements can provide information about injection, transport, defect-dependent trapping, detrapping, and recombination processes in thin layers of semiconductor or insulator devices.[8–12] In addition, wavelength-dependent EFISH measurements can identify and measure thresholds in multiphoton carrier injection processes from which band offsets and defect trap levels can be obtained.[13] These results suggest that one may be able to use the SHG technique, which is contactless and noninvasive, as an alternative to conventional electrical measurements for *in situ* monitoring of the properties of thin dielectric layers. In this paper we report the results of measurements of electric-field-induced second-harmonic generation from the $Si/SiO_2$ system as a function of temperature. The goal of this research is to understand the physical processes associated with the creation of the photoinduced electric field and extend our knowledge of the effect of temperature on the nonlinear optical susceptibilities at the interface. The two-color EFISH technique, used in this study, enables us to distinguish the unique contributions of each of these physical processes. Unlike single-beam experiments, the photoinduced electric-field creation process in two-color experiments can be completely decoupled from the probing technique, making it an extremely sensitive tool for monitoring the transport of carriers.

The two-color electric-field-induced second-harmonic generation technique allows us to experimentally separate optical second-harmonic generation and carrier injection processes and to directly follow the dynamics of photoexcited charge carriers. The experimental setup used in the present study was similar to the one used by Marka *et al.*[8] We used a 150 fs Ti:sapphire oscillator set to 800 nm (1.55 eV) as a probe of the second-harmonic generation response. The intensity of the beam was sufficiently low (the peak intensity was around 3.3 $GW/cm^2$) such that the probe laser beam did not contribute significantly to carrier injection and therefore to charge trapping. The second-harmonic signal (at 400 nm) was optically separated from the fundamental beam by a prism and measured by a photomultiplier tube. Both fundamental and second-harmonic beams were *p* polarized. A tunable optical parametric generator (OPG) was used as a pump laser. The wavelength of the *s*-polarized OPG was set to 540 nm (2.3 eV), and its intensity was kept at a level that ensured creation of the electric field by internal photoemission, without significantly heating the sample. In our case, the pump-laser peak intensity was about 40 $GW/cm^2$. The measurements were performed on thermally grown 4.2-nm-thick $SiO_2$ deposited on Si(100). At this oxide thickness, the photoinjected electrons can reach the surface with a high probability, giving rise to a large easily detectable time-dependent EFISH signal resulting from changes in the electric field at the interface. This oxide is also thick enough that electron tunneling from the oxide surface back to the silicon (in the absence of assistance from defects or impurities) is negligible on the time scale of the measurements. The sample was oriented such that the azimuthal angle of the plane of incidence was along the (110) direction. The sample was kept in a continuously flowing helium cryostat, which allowed us to perform measurements at temperatures ranging from 4.3 to 296 K. Because the interfacial electric field sensed by EFISH in these films arises from electron trapping by ambient physisorbed oxygen at the surface of the $SiO_2$, its saturation level may be oxygen pressure dependent. The saturation level of photoinduced electric-field-induced second-harmonic generation decreases with decreasing pressure and vanishes around $1\times10^{-10}$ Torr.[14] In our experiment the pressure in the cryostat at room temperature was kept at $\sim2\times10^{-5}$ Torr to ensure that the oxygen coverage was saturated which resulted in a constant surface trap density.

 

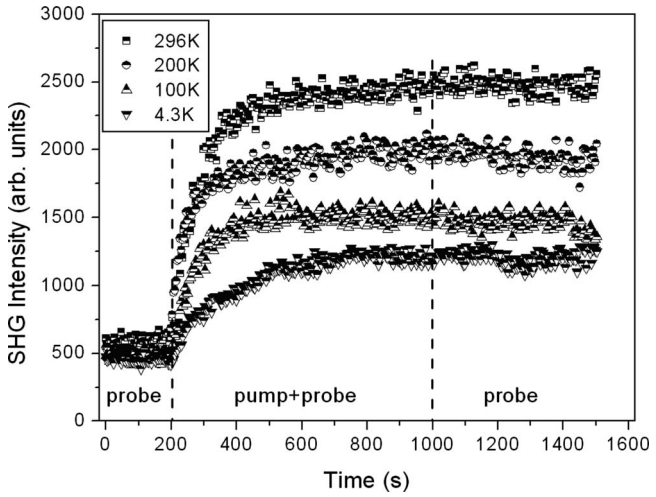


FIG. 1. Time-dependent EFISH measurements from the $Si(100)/SiO_2(4.2\ nm)$ system at different temperatures.

The experimental procedure was carried out in three stages (Fig. 1). For the first 200 s only the probe laser was on. That made it possible to record the SHG intensity due to the second-order optical nonlinear susceptibility without any significant charge accumulation on the $SiO_2$ surface. During the second stage of the experiment (800 s), both pump and probe lasers were on. The pump beam was responsible for the creation of a photoinduced electric field, arising from two-photon excitation of the electrons from the silicon valence band to the conduction band of the $SiO_2$, and then the transport and subsequent trapping of the electrons at the surface of the oxide. The probe laser detected the increase in the electric field at the $Si/SiO_2$ interface as an increase in the measured SHG intensity.

The pump photon energy of 2.3 eV makes the electron injection from the Si valence band to the $SiO_2$ conduction band a two-photon process. On the other hand, the hole injection from the Si valence band to the $SiO_2$ valence band is a three-photon process, which is a higher-order process. Hence, the hole injection is much less probable than electron injection. Also, the mobility of holes in $SiO_2$ is about $1 \times 10^{-10}$ $m^2/V$ s much lower than electron mobility, which is about $2 \times 10^{-3}$ $m^2/V$ s.[15,16] Therefore, most holes remain in the vicinity of the $Si/SiO_2$ interface mostly in Si. This is in contrast to the electrons that are free to move to the surface of the $SiO_2$ and be trapped by the ambient oxygen.

During the third and last stages of the experiment, the pump laser was turned off, leaving the probe laser to monitor the electric field arising from the trapped electrons and holes. In our case, no significant back tunneling of the electrons through the oxide was observed at any of the temperatures used in this experiment, indicating a relatively low density of defects and impurities with energy levels within the $SiO_2$ band gap.

It has been reported that heating effects due to the femtosecond laser pulses can affect the SHG response in some cases.[17] One can easily estimate if this affects the measurements presented here. We first consider possible heating due to the pump laser. As can be seen in Fig. 1, after the pump beam is blocked, the EFISH saturation intensity remains at the same level. This is an indication that not only is electron tunneling from the oxide surface back to the silicon negligible but also that heating effects are negligible. A similar test was performed with the probe laser. Blocking and unblocking the probe beam showed no variation in SHG response due to possible heating or cooling of the sample.

## II. TEMPERATURE DEPENDENCE OF EFISH INTENSITY

The time-dependent EFISH signals from $Si/SiO_2$ at four different temperatures are shown in Fig. 1. It is clear that the SHG intensities, both initial and saturation values, increase with temperature. Previous temperature-dependent studies showed that the reflectivity differs by less than about 2% in the temperature range between 10 and 300 K.[18,19] This small difference is negligible compared to the difference of SHG intensities, which is greater than 40%. Thus, in this paper, we attribute changes in SHG intensities solely to temperature variations in the nonlinear susceptibilities.

The intensity of the electric-field-induced second-harmonic generation can be expressed as

$$I^{(2\omega)}(t) = |\chi^{(2)} + \chi^{(3)}E(t)|^2 (I^{(\omega)})^2, \tag{1}$$

where $I^{(\omega)}$ and $I^{(2\omega)}(t)$ are the intensities of the fundamental and the time-dependent SHG beams, respectively. Here $\chi^{(2)}$ is the second-order susceptibility, $E(t)$ is a photoinduced electric field present at the interface, and $\chi^{(3)}$ is the third-order nonlinear susceptibility.

It should be pointed out that the probe laser is set at a wavelength of 800 nm with a photon energy of 1.55 eV in our experiment. Si is an indirect band-gap semiconductor and the interband absorption spectrum shows that the absorption coefficient is very low at 1.55 eV.[20] Also, $SiO_2$ has a band gap of about 9 eV and it is transparent to a laser with photon energy of 1.55 eV. Therefore, Si and $SiO_2$ are effectively lossless media in our experiments and both $\chi^{(2)}$ and $\chi^{(3)}$ are real numbers.[21]

For centrosymmetric systems, such as crystalline silicon, the second-order nonlinear optical susceptibility vanishes under the dipole approximation but at the interface the symmetry is broken and second-order nonlinear processes are allowed. The contribution from the quadrupole bulk contribution is allowed. However, the bulk oxide third-order susceptibility is about $1 \times 10^4$ smaller than for bulk Si.[22] Also, there is no electric field present in the bulk Si other than the optical field. Thus, both $\chi^{(2)}$ and $\chi^{(3)}$ represent only the $Si/SiO_2$ interface.

The measured temperature dependence of the second-order susceptibility increases with temperature as shown in Fig. 2(a). This observation is consistent with previous results obtained by Suzuki *et al.*[23] and Dadap *et al.*[24] for higher temperatures. A broad peak of two-photon $E_1$ resonance in the silicon second-harmonic spectrum red shifts and broadens with increasing temperature. This thermally enhanced SHG arising from results from a combination of (1) the differential thermal expansion of the lattice at the interface resulting in a change in the energy-band structure[4,25] and (2) the renormalization of band energies arising from the electron-phonon interaction.[25,26]

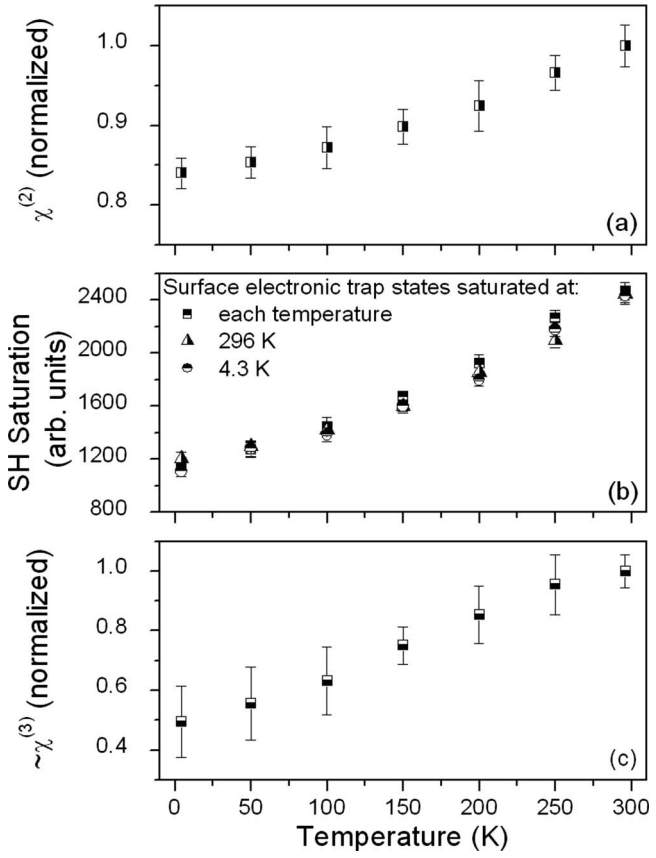


FIG. 2. Temperature dependence of: (a) the second-order nonlinear susceptibility; (b) the photoinduced EFISH saturation intensity; and (c) the third-order nonlinear optical susceptibility.

The electric field in Eq. (1) arises from charge separation due to multiphoton excitation of electrons in the valence band of silicon above the conduction band of $SiO_2$, the subsequent transport of these electrons across the oxide, and trapping at the surface of the oxide by ambient oxygen.[14,27] Van Driel and coworkers suggest that ambient oxygen captures the electrons at the surface of the $SiO_2$ because of the high electron affinity of the oxygen. The electrons and oxygen attract each other in a harpooning reaction in the vicinity of the $SiO_2$ or ambient interface and then attach to or even penetrate the positively charged solid.[28] It also has been shown that the saturation EFISH intensity varies with the oxygen pressure because of the change in the number of available electronic trap states for photoinjected electrons. The combined measurements of photoemission currents and the contact-potential difference confirm that photoinduced gas-assisted charging gives rise to the observed second-harmonic generation induced by internal photoemission in thin $Si/SiO_2$ films.[29] For a 1.6 nm oxide the maximum near-interface electric field in the oxide was estimated to be $\sim$0.6 MV/cm, giving a surface charge density of $5 \times 10^{11}$ $cm^{-2}$ (assuming an oxide dielectric constant of $\sim$3.8).

The value of EFISH saturation intensity is determined not only by the electric field present at the interface but also by the second- and third-order optical nonlinear susceptibilities as shown in Eq. (1). Photoinduced electric fields are a measure of the surface electron density: $E(t)=\sigma(t)/\varepsilon_{Si}$, where the surface electron density $\sigma(t)$ is proportional to the number of filled electronic trap states at the surface of the oxide. This photoinduced electric field at the $Si/SiO_2$ interface is proportional to the number of filled electronic trap states and can be expressed by a rate equation.[8,13] In the case of the system where only electron dynamics contribute to the electric field, this can be written as

$$\frac{dn_e}{dt} = \frac{(n_{0e} - n_e)}{\tau^e_{\text{trapping}}} - \frac{n_e}{\tau^e_{\text{detrapping}}}, \tag{2}$$

where $n_{0e}$ is the initial number of the unfilled electronic trap states and $1/\tau^e_{\text{trapping}}$ is the trapping rate of states due to electron injection caused by the pump laser beam (as mentioned above, electron injection due to the probe laser can be neglected). The value of $1/\tau^e_{\text{detrapping}}$ is related to the lifetime of surface electronic trap states. The last term in Eq. (2) can be neglected because for the 4.2-nm-thick $SiO_2$, the value of $\tau^e_{\text{detrapping}}$ is significantly greater than $\tau^e_{\text{trapping}}$. In that case, the number of filled electronic surface trap states can be described by the simplified expression

$$n_e(t) = n_{0e}(1 - \exp[-t/\tau^e_{\text{trapping}}]). \tag{3}$$

By introducing Eq. (3) into Eq. (1), it can be shown that the difference between the initial and saturation intensities of photoinduced EFISH is a function of the second- and third-order optical nonlinear susceptibilities and the number of available electronic trap states,

$$\Delta I^{(2\omega)} = I^{(2\omega)}(\infty) - I^{(2\omega)}(0) = [(\chi^{(3)} n_e/\varepsilon_{Si})^2 + 2\chi^{(2)}\chi^{(3)} n_e/\varepsilon_{Si}] \times (I^{\omega})^2. \tag{4}$$

From Eq. (3), it is clear that when the saturation of the second-harmonic intensity is reached, the number of filled electronic trap states $n_e$ is the same as the initial number of available electronic trap states at the surface $n_{0e}$. Thus, we replace $n_{0e}$ with $n_e$ in Eq. (4).

Previous temperature-dependent studies showed that the Si dielectric constant $\varepsilon_{Si}$ differs by about 4% in the temperature range between 10 and 300 K.[18,19] It can be treated as temperature independent in our experiment. Our data clearly show that $\chi^{(2)}$ changes with temperature. To explain the differences in the EFISH saturation intensity values, the temperature dependences of the third-order optical nonlinear susceptibility $\chi^{(3)}$ and number of filled electronic trap states must be investigated. The two-color EFISH technique allows us to saturate surface electronic trap states at a given temperature by the pump laser. Once the saturation of the EFISH is reached, the pump laser can be blocked, and we can directly follow the change in saturation intensity as a function of temperature using the probe laser only. This ensures that no additional electric field is created when the temperature is changed. Figure 2(b) shows values of EFISH saturation intensities as a function of temperature. First, the EFISH saturation was obtained at 296 K and pump laser was turned off [Fig. 2(b), triangles]. Then the temperature was gradually decreased down to 4.3 K while the second-harmonic intensity was monitored by the probe laser. A similar measurement was performed for the saturation obtained at 4.3 K

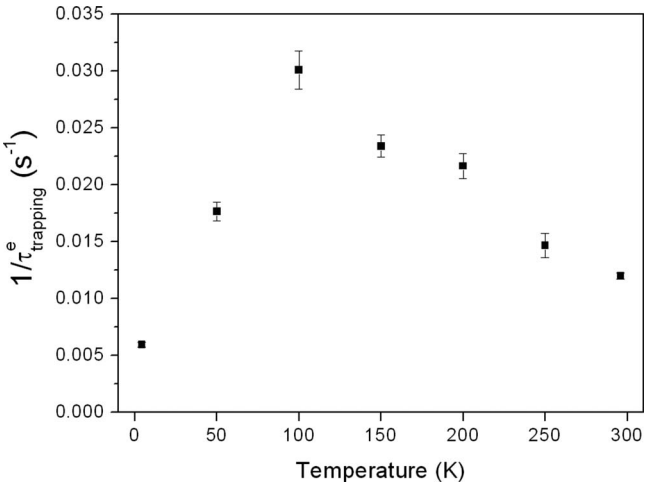


FIG. 3. Temperature dependence of the trapping rate $(1/\tau^{e}_{\text{trapping}})$.

followed by increasing temperature [Fig. 2(b), circles]. Those results were compared to the values obtained by filling the surface electronic trap states at each temperature independently [Fig. 2(b), squares]. All of these values are comparable within experimental error. *We conclude that the photoinduced electric field, which is related to the number of filled surface electronic trap states, is independent of temperature.* This shows that the increase in EFISH saturation intensity, as shown in Fig. 1, is due entirely to the temperature-dependent variations in $\chi^{(2)}$ and $\chi^{(3)}$, and not due to changes in the value of the photoinduced electric field.

Since the temperature dependence of the second-order nonlinear susceptibility has been determined in our experiments, and the number of filled electronic trap states and thereby the electric field was shown to be constant, it is possible to find the temperature dependence of the third-order nonlinear susceptibility using Eq. (4). The third-order nonlinear susceptibility was found to exhibit a nearly linear behavior as shown in Fig. 2(c). One can represent the observed SHG intensities as far-field radiation from dipoles driven in a nonharmonic fashion by the incident electric field.[30] The photoinduced electric field created at the interface will change this potential giving rise to an additional SH signal. The third-order nonlinear susceptibility represents the coupling between the electric field produced by the incident light and the photoinduced electric field present at the interface.

## III. TRANSPORT OF PHOTOEXCITED ELECTRONS ACROSS THE OXIDE

In addition to the thermally dependent EFISH intensity, the rise time of the photoinduced electric field is a function of temperature. This rise time reflects the combined effects of temperature on charge-carrier excitation in silicon, injection of electrons at the $Si/SiO_2$ interface, transport through the oxide, and trapping of electrons at the surface of the $SiO_2$. Figure 3 shows the temperature dependence of the trapping rate $(1/\tau^{e}_{\text{trapping}})$. It peaks around $T=120$ K with nonsymmetric behavior. It should be pointed out that our previous analysis of the pump-power-dependent measurements have shown that at a pump photon energy of 2.3 eV, electron excitation from the silicon valence band to above the conduction band of $SiO_2$ is a two-photon process at all temperatures. This is an indication that although the band gap of the Si increases at low temperatures [the band gap is 1.17 eV at 4.3 K and 1.12 eV at 300 K (Ref. 15)], the band offset at the $Si/SiO_2$ interface remains less than 4.6 eV.

At higher temperatures above the peak temperature ~120 K, electron-phonon scattering is likely to be responsible for the decrease in the transport rate as a function of increasing temperature.[31] This is because the density of phonons in solids increases with temperature. Thus, the scattering time due to this mechanism will decrease with temperature as will the transport rate across the oxide.

Note that the observed trapping rate, $1/\tau^{e}_{\text{trapping}}$, increases as a function of temperature at temperatures below ~120 K. We attribute this behavior to a combination of two effects. First, the absorption coefficient of Si is known to increase as the temperature increases[15] due primarily to electron-hole pair creation. This results in an increased electron-hole pair-production rate with temperature, which subsequently increases the injection of electrons into the $SiO_2$ conduction band. Second, the $SiO_2$ relative dielectric constant increases with temperature,[21] which makes the net electric field inside $SiO_2$ decrease with increased temperature. Therefore, higher temperature assists the electron transport inside the oxide. These two effects together result in the observation that $1/\tau^{e}_{\text{trapping}}$ increases with increasing temperature at temperatures below 120 K. The nonsymmetric behavior of $1/\tau^{e}_{\text{trapping}}$ at low and high temperatures results from a competition between these effects and electron-phonon scattering.

## IV. SUMMARY

In summary, the temperature dependence of electric-field-induced second-harmonic generation in the $Si/SiO_2$ system was studied to gain better understanding of the physical processes associated with the creation of a photoinduced electric field. The intensity of time-dependent EFISH is a function of the second- and third-order optical nonlinear susceptibilities and the densities of occupied surface electron traps. The results reveal that the second-order nonlinear optical susceptibility increases with temperature. This may be qualitatively related to the thermal expansion of the lattice. Our measurements also show that the changes in the EFISH saturation intensity are due to temperature-dependent variations in both the second-order nonlinear susceptibility $\chi^{(2)}$ and the third-order nonlinear susceptibility $\chi^{(3)}$. Under our experimental conditions, the number of filled electronic trap states at the surface of the oxide, related to the ambient oxygen, is temperature independent. Consequently, the photoinduced electric field does not change over our temperature range. In addition, our measurements show that the temperature dependence of the trapping rate $1/\tau^{e}_{\text{trapping}}$ is a combination effect of electron-phonon scattering and of the temperature dependence of the Si absorption coefficient and the $SiO_2$ dielectric constant. These studies provide insight into the dy-

namics of excited carriers in the $Si/SiO_2$ system.

## ACKNOWLEDGMENTS

This work was supported by grants from the Air Force Office of Scientific Research through the Multidisciplinary University Research Initiative program, the Advanced Carbon Nanotechnology Program, and the Department of Energy. We also acknowledge valuable discussions with L. C. Feldman.

[1] C. H. Bjorkman, T. Yasuda, C. E. Shearon, Y. Ma, G. Lucovsky, U. Emmerichs, C. Meyer, K. Leo, and H. Kurz, J. Vac. Sci. Technol. B **11**, 1521 (1993).
[2] J. I. Dadap, B. Doris, Q. Deng, M. C. Downer, J. K. Lowell, and A. C. Diebold, Appl. Phys. Lett. **64**, 2139 (1994).
[3] S. T. Cundiff, W. H. Knox, F. H. Baumann, K. W. Evans-Lutterodt, and M. L. Green, J. Vac. Sci. Technol. A **16**, 1730 (1998).
[4] S. V. Govorkov, N. I. Koroteev, G. I. Petrov, I. L. Shumay, and V. V. Yakovlev, Appl. Phys. A: Solids Surf. **50**, 439 (1990).
[5] A. Y. Abdullaev, S. V. Govorkov, P. K. Kashkarov, N. I. Koroteev, G. I. Petrov, and I. L. Shumai, Fiz. Tverd. Tela (S.-Peterburg) **29**, 1898 (1987).
[6] B. Jun *et al.*, IEEE Trans. Nucl. Sci. **51**, 3231 (2004).
[7] Y. D. Glinka *et al.*, Phys. Rev. B **65**, 193103 (2002).
[8] Z. Marka, R. Pasternak, R. G. Albridge, S. N. Rashkeev, S. T. Pantelides, N. H. Tolk, B. K. Choi, D. M. Fleetwood, and R. D. Schrimpf, J. Appl. Phys. **93**, 1865 (2003).
[9] R. Pasternak *et al.*, IEEE Trans. Nucl. Sci. **50**, 1929 (2003).
[10] T. Scheidt, E. G. Rohwer, H. M. von Bergmann, and H. Stafast, Eur. Phys. J.: Appl. Phys. **27**, 393 (2004).
[11] V. Fomenko, E. P. Gusev, and E. Borguet, J. Appl. Phys. **97**, 083711 (2005).
[12] Y. V. White, X. Lu, R. Pasternak, N. H. Tolk, A. Chatterjee, R. D. Schrimpf, D. M. Fleetwood, A. Ueda, and R. Mu, Appl. Phys. Lett. **88**, 062102 (2006).
[13] Z. Marka, R. Pasternak, S. N. Rashkeev, Y. Jiang, S. T. Pantelides, N. H. Tolk, P. K. Roy, and J. Kozub, Phys. Rev. B **67**, 045302 (2003).
[14] J. Bloch, J. G. Mihaychuk, and H. M. vanDriel, Phys. Rev. Lett. **77**, 920 (1996).
[15] S. M. Sze, *Physics of Semiconductor Devices* (Wiley, New York, 1981).
[16] G. E. McGuire, *Semiconductor Materials and Process Technology Handbook* (Noyes, Park Ridge, NJ, 1988).
[17] J. I. Dadap, X. F. Hu, N. M. Russell, J. G. Ekerdt, J. K. Lowell, and M. C. Downer, IEEE J. Sel. Top. Quantum Electron. **1**, 1145 (1995).
[18] G. E. Jellison and F. A. Modine, Phys. Rev. B **27**, 7466 (1983).
[19] B. J. Frey, D. B. Leviton, and T. J. Madison, in *Astronomical Telescopes 2006*, edited by J. A. Eli Atad-Ettedgui (Dietrich Lemke, Orlando, FL, 2006).
[20] E. D. Palik, *Handbook of the Optical Constants of Solids* (Academic, San Diego, 1985).
[21] M. Fox, *Optical Properties of Solids* (Oxford University Press, New York, 2001).
[22] J. G. Mihaychuk, N. Shamir, and H. M. van Driel, Phys. Rev. B **59**, 2164 (1999).
[23] T. Suzuki, S. Kogo, M. Tsukakoshi, and M. Aono, Phys. Rev. B **59**, 12305 (1999).
[24] J. I. Dadap, Z. Xu, X. F. Hu, M. C. Downer, N. M. Russell, J. G. Ekerdt, and O. A. Aktsipetrov, Phys. Rev. B **56**, 13367 (1997).
[25] P. Lautenschlager, P. B. Allen, and M. Cardona, Phys. Rev. B **31**, 2163 (1985).
[26] P. B. Allen and V. Heine, J. Phys. C **9**, 2305 (1976).
[27] J. G. Mihaychuk, J. Bloch, Y. Liu, and H. M. Vandriel, Opt. Lett. **20**, 2063 (1995).
[28] R. D. Levine and R. B. Bernstein, *Molecular Reaction Dynamics and Chemical Reactivity* (Oxford University Press, Oxford, 1987).
[29] N. Shamir and H. M. van Driel, J. Appl. Phys. **88**, 909 (2000).
[30] J. F. T. Wang, G. D. Powell, R. S. Johnson, G. Lucovsky, and D. E. Aspnes, J. Vac. Sci. Technol. B **20**, 1699 (2002).
[31] M. V. Fischetti and D. J. Dimaria, Solid-State Electron. **31**, 629 (1988).